



Gamow-Teller transitions from ^{56}Ni

Masaki Sasano

Uesaka spin-isospin laboratory

RIKEN Nishina Center

M. Sasano,^{1,2} G. Perdikakis,^{1,2} R.G.T. Zegers,^{1,2,3} Sam M. Austin,^{1,2} D. Bazin,¹ B. A. Brown,^{1,2,3} C. Caesar,⁴ A. L. Cole,⁵ J.M. Deaven,^{1,2,3} N. Ferrante,⁶ C.J. Guess,^{7,2} G. W. Hitt,⁸ H. Honma,⁹ R. Meharchand,^{1,2,3} F. Montes,^{1,2} J. Palardy,⁶ A. Prinke,^{1,2,3} L. A. Riley,⁶ H. Sakai,¹⁰ M. Scott,^{1,2,3} A. Stolz,¹ T. Suzuki,^{11,12,13} L. Valdez,^{1,2,3} and K. Yako¹⁴

¹National Superconducting Cyclotron Laboratory, Michigan State University, East Lansing, MI 48824-1321, USA

²Joint Institute for Nuclear Astrophysics, Michigan State University, East Lansing, MI 48824, USA

³Department of Physics and Astronomy, Michigan State University, East Lansing, MI 48824, USA

⁴GSI Darmstadt, Helmholtz-Zentrum für Schwerionenforschung, D-64291, Darmstadt, Germany

⁵Physics Department, Kalamazoo College, Kalamazoo, MI 49006, USA

⁶Department of Physics and Astronomy, Ursinus College, Collegeville, Pennsylvania 19426, USA

⁷Department of Physics, University of Massachusetts Lowell, Lowell, MA 01854, USA

⁸Khalifa University of Science, Technology & Research, 127788 Abu Dhabi, UAE

⁹Center for Mathematical Sciences, University of Aizu, Aizu-Wakamatsu, Fukushima 965-8580, Japan

¹⁰RIKEN Nishina Center, Wako, 351-0198, Japan

¹¹Department of Physics, College of Humanities and Sciences,

Nihon University, Sakurajosui 3-25-40, Setagaya-ku, Tokyo 156-8550, Japan

¹²Center for Nuclear Study, University of Tokyo, Hirosawa, Wako-shi, Saitama 351-0198, Japan

¹³National Astronomical Observatory of Japan, Mitaka, Tokyo 181-8588, Japan

¹⁴Department of Physics, University of Tokyo, Tokyo, 113-0033, Japan

Charge-Exchange (CE) reactions: a tool for studying Gamow-Teller strengths

Gamow-Teller transition

$$\Delta T=1, \Delta S=1, \Delta L=0$$

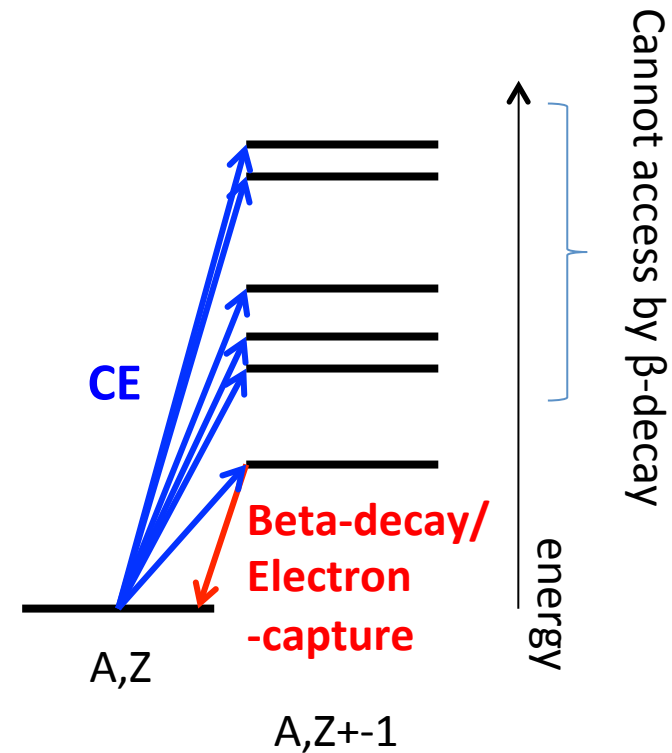
induced by $\sigma \tau_{\pm}$

strength : **B(GT)**

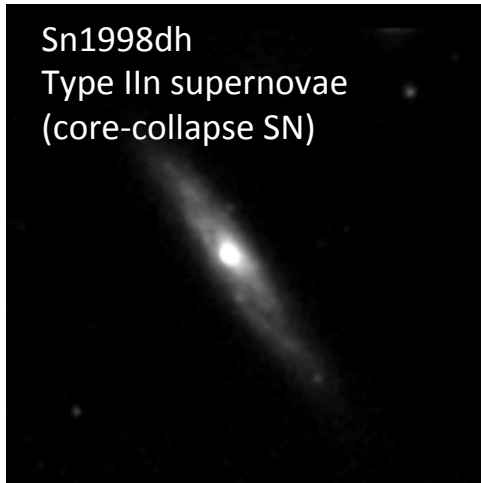
→ allowed β -decay

CE reaction at intermediate energies,
e.g. (p,n) reaction

$$\left(\frac{d\sigma}{d\Omega}(q=0) \right)_{(p,n)} = \hat{\sigma} B(GT)$$



Weak reactions in astrophysics



Core-Collapse (Type II) Supernovae

- Collapse of massive star at the end of burning cycle
- electron-capture (EC) on Fe-region nuclei
 - reduces electron pressure
 - neutrinos by EC carry away energy from the star
→ collapse accelerates
- affects the mass interior to the shockwave

Thermonuclear (Type Ia) Supernovae

- source of large fraction of Iron group nuclei in the universe
- thermonuclear explosions of accreting white dwarfs in binary systems **Not well understood.**

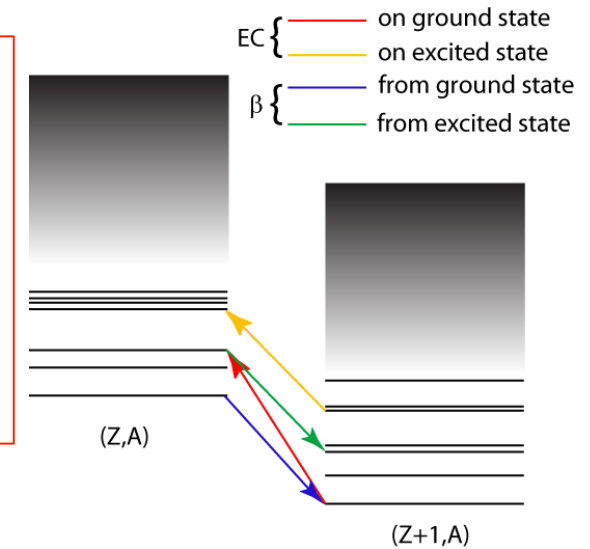


- ECs strongly affect the flame propagation after ignition
- If ECs are well understood → models can be much better constrained

Key ingredient : Electron capture in Fe-region nuclei

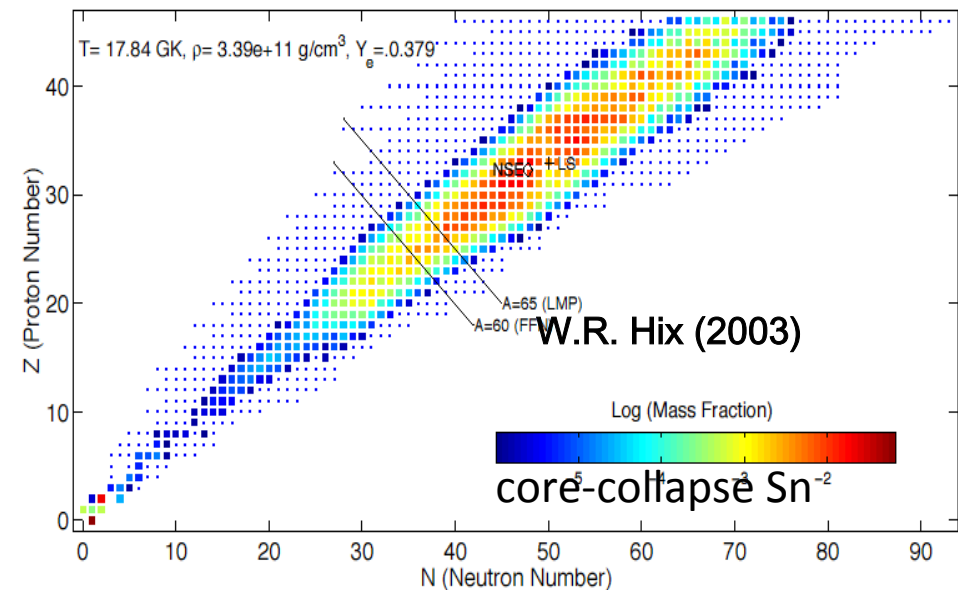
Weak reactions (electron capture) in supernovae

- Key ingredient: **Gamow-Teller strengths**
- Many nuclei play a role (A-40-120)
- Majority are unstable
- excitation can take place from excited nuclear states



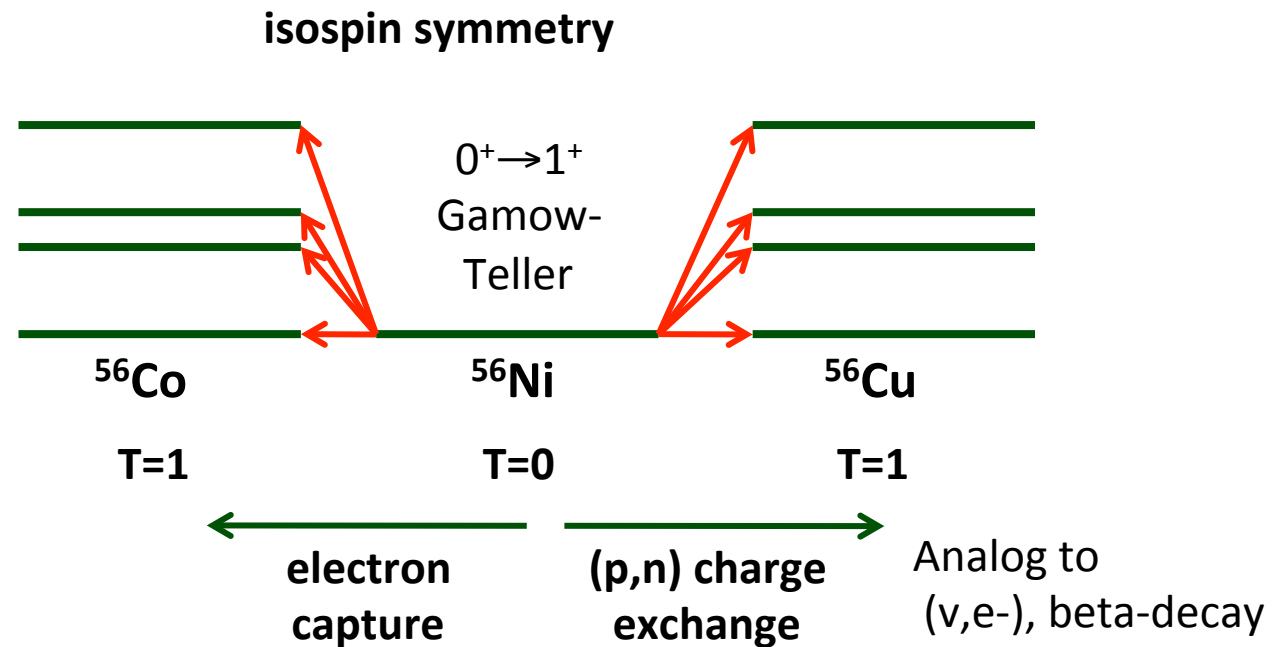
Impossible to measure even a sizeable fraction of cases

- Test theory with cases that constrain key model parameters
- Measure nuclei that are particularly abundant in supernovae



Electron capture in ^{56}Ni

One of the important cases
in core collapse super novae of massive stars
(Phys. Rev. Lett. 86, 1678 (2001))



$B(\text{GT})$ measured by the (p,n) reaction is directly
connected with the EC rate.

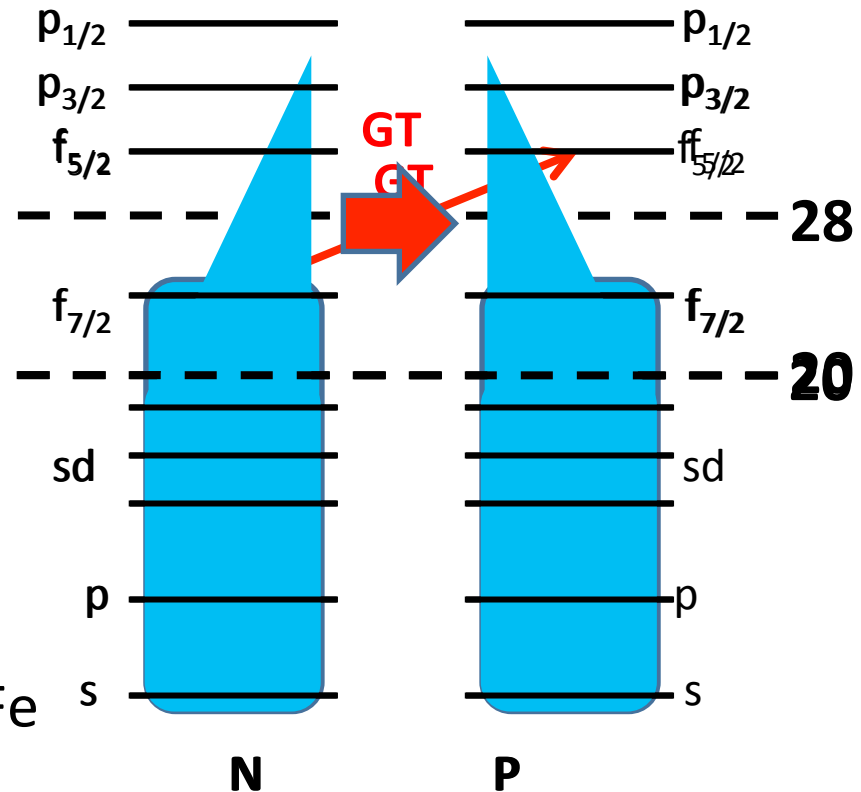
^{56}Ni is a key nucleus in Fe region

^{56}Ni ($Z=N=28$)

- independent particle model
→ ^{56}Ni is doubly magic
- Large p-n residual interaction
→ ^{56}Ni is not magic
- **GT strength from ^{56}Ni**
→ key to bench mark nuclear model used for weak rates in the Fe region



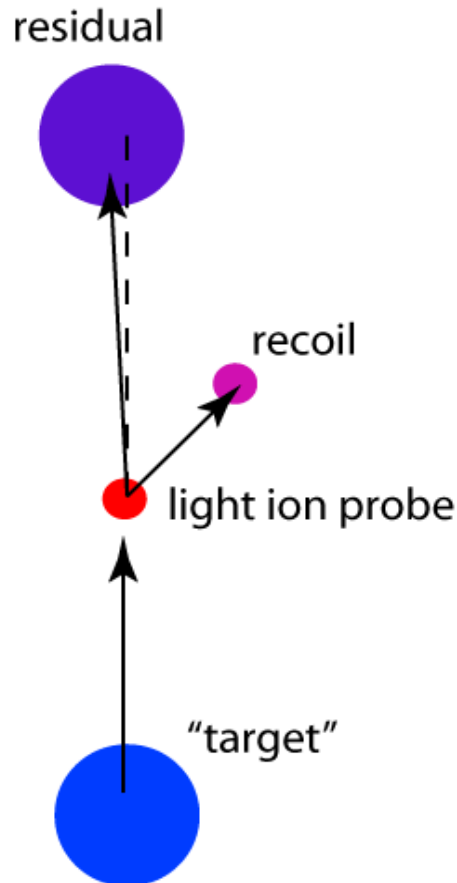
Experimentally, challenging!



f7/2 70% in ^{56}Ni (GXPF1A, KB3G)
(e.g., Honma et al., Phys. Rev. C 69, 034335 (2004))

Existing CE studies using RI beams

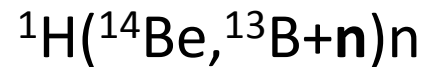
inverse kinematics



(Zegers et al., Phys. Rev. Lett. 104, 212504 (2010))



(Meharchand et al., to be published)

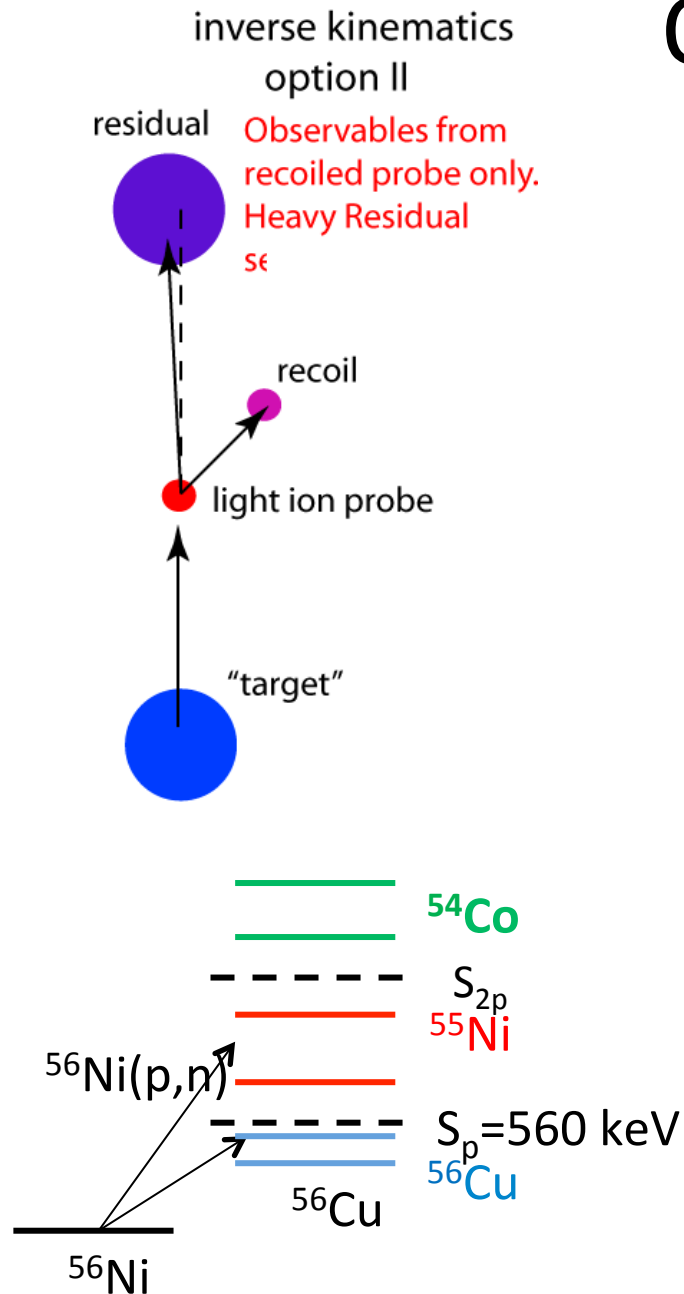


(Satou et al., Phys. Lett. B 697 (2011) 459-462.)

→ Only several low-lying states and light nuclei

(For high E_x /heavier nuclei, to analyze the residue decays becomes difficult)

Our method



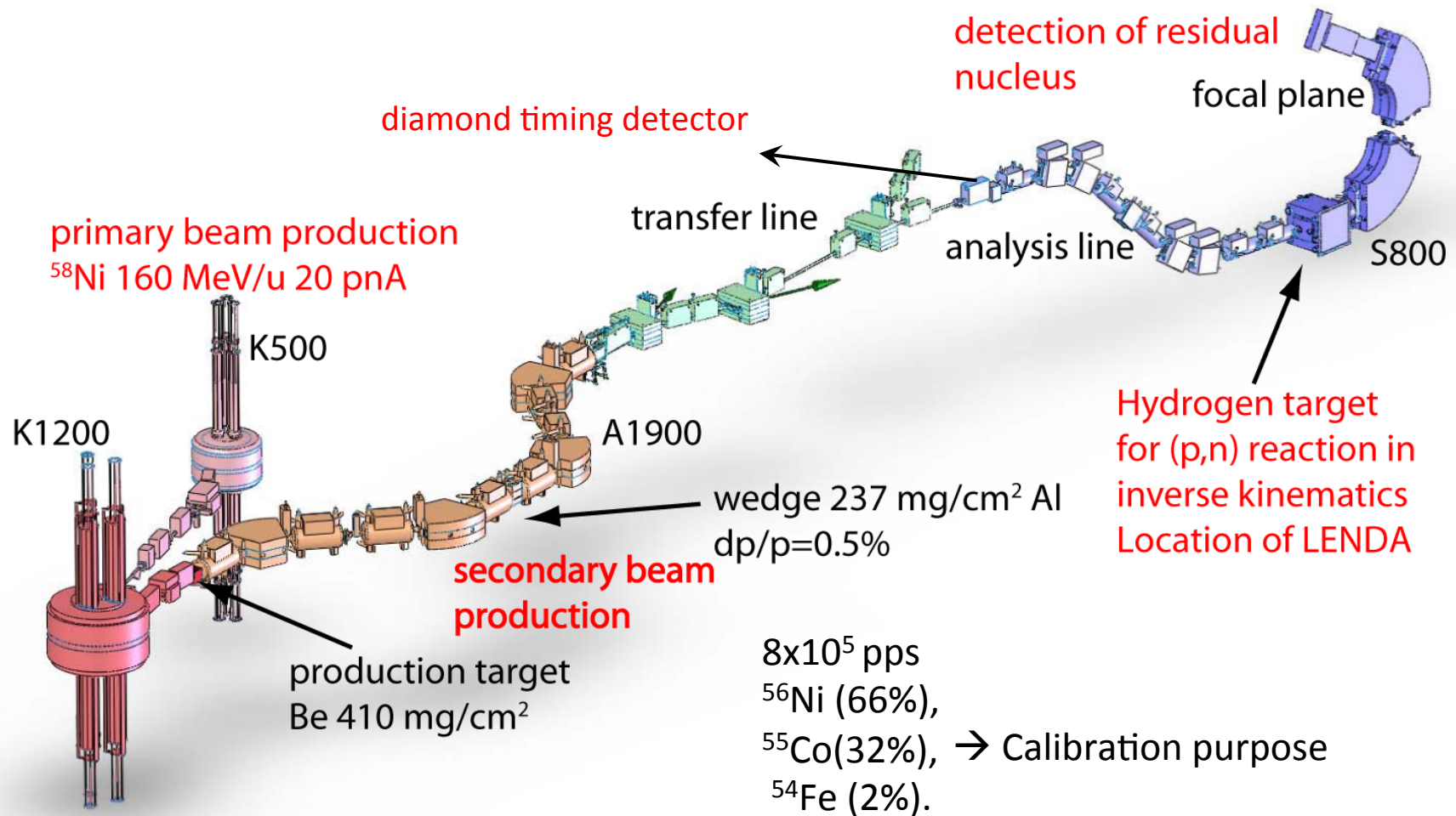
Missing mass spectroscopy by the detection of the recoil neutron

Advantages

- target can be thick (neutron recoil)
 - high luminosity
 - even with unstable beams
 - with low intensities
- All kinematic information from measurement of the neutron (two-body kinematics)
 - simple measurement and analysis, compared to invariant mass method
- Heavy fragment serves as tag for CE reaction
 - branching ratio of the particle decay

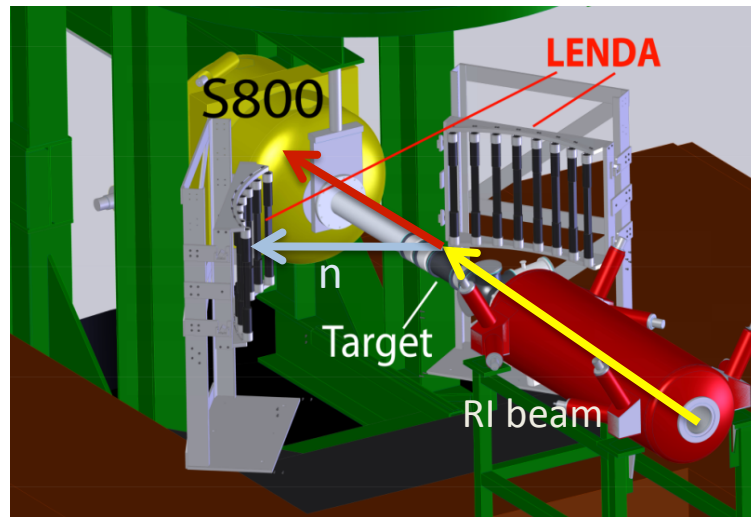
Can be applied to any mass region and to any excitation energy

^{56}Ni beam production and experiment overview



National Superconducting Cyclotron Laboratory,
Michigan State University

Set up of LENDA



Low Energy Neutron Detector Array (LEND A)

neutron detection

Plastic scintillator

24 bars 2.5x4.5x30cm

$150 \text{ keV} < E_n < 10 \text{ MeV}$

$\Delta E_n \sim 5\%$ $\Delta \theta_n < 2^\circ$

efficiency 15-40%

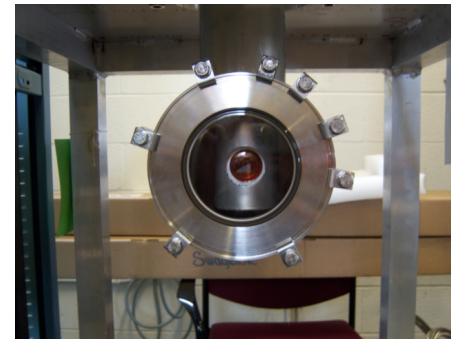
Flight path : 1 m



Neutron energy & angles



Excitation energy
& reaction scattering angles



Liquid Hydrogen target

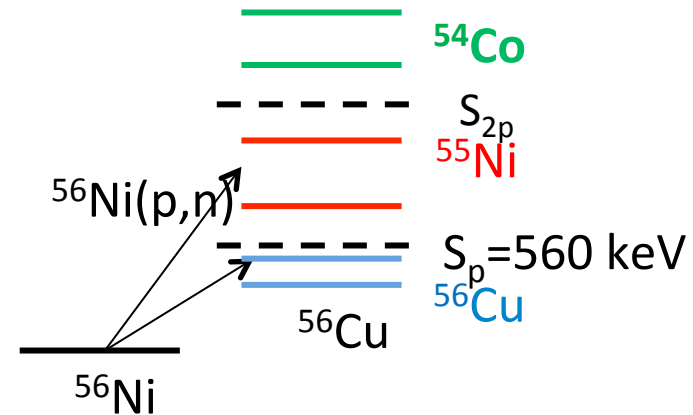
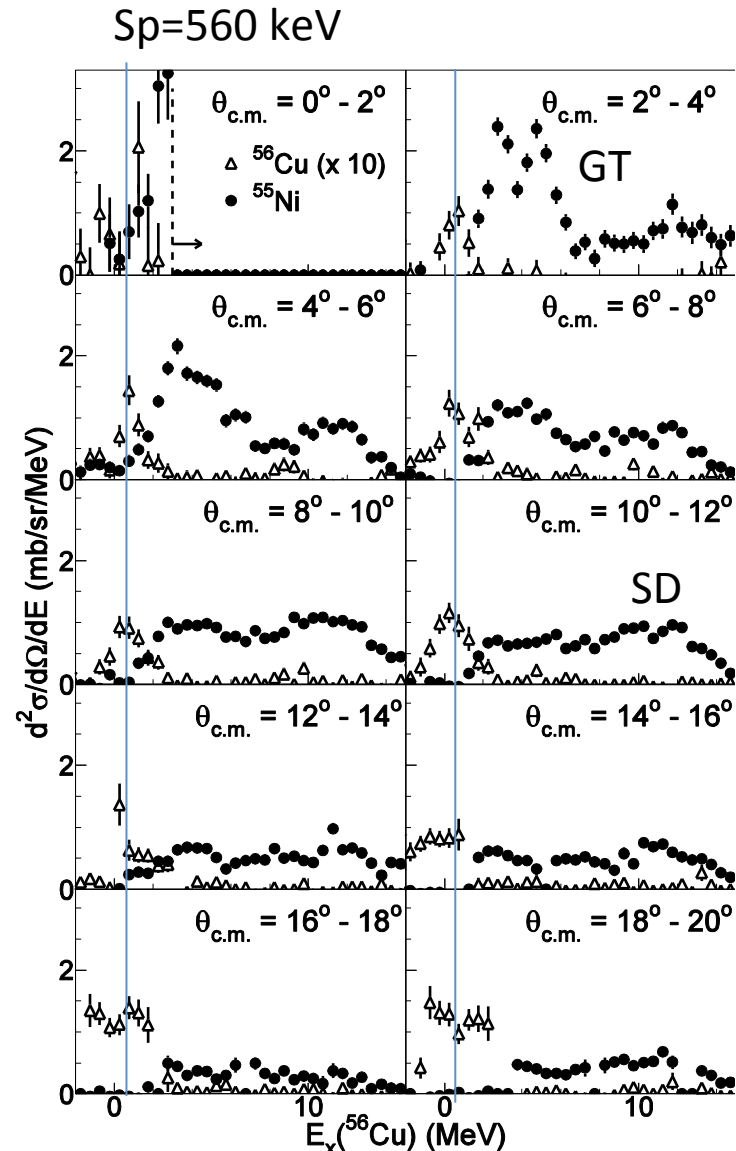
"proton" target

65 mg/cm^2 ($\sim 7 \text{ mm}$)

$\sim 3.5 \text{ cm}$ diameter

$T=20 \text{ K}$ $\sim 1 \text{ atm}$

Double differential cross sections



Two bumps at 3 and 5 MeV
 with forward angle peaks (GT: $\Delta L=0$)

A bump around 12 MeV
 \rightarrow Peak around 10-12 degrees
 \rightarrow Spin dipole ($\Delta L=1$)

States without proton emission
 \rightarrow Peak at most backward angle
 \rightarrow Higher multipoles ($\Delta L>1$)

To extract GT component quantitatively
 \rightarrow Multipole decomposition

Multipole decomposition analysis

Experimental angular distribution for each energy bin



Fit with linear combination of calculated angular distribution

$$\sigma_{exp}(\theta, cm) \approx \sum_{\Delta L=0}^{\infty} a_{\Delta L} \sigma_{\Delta L}; \sigma_{\Delta L}(\theta, cm)$$

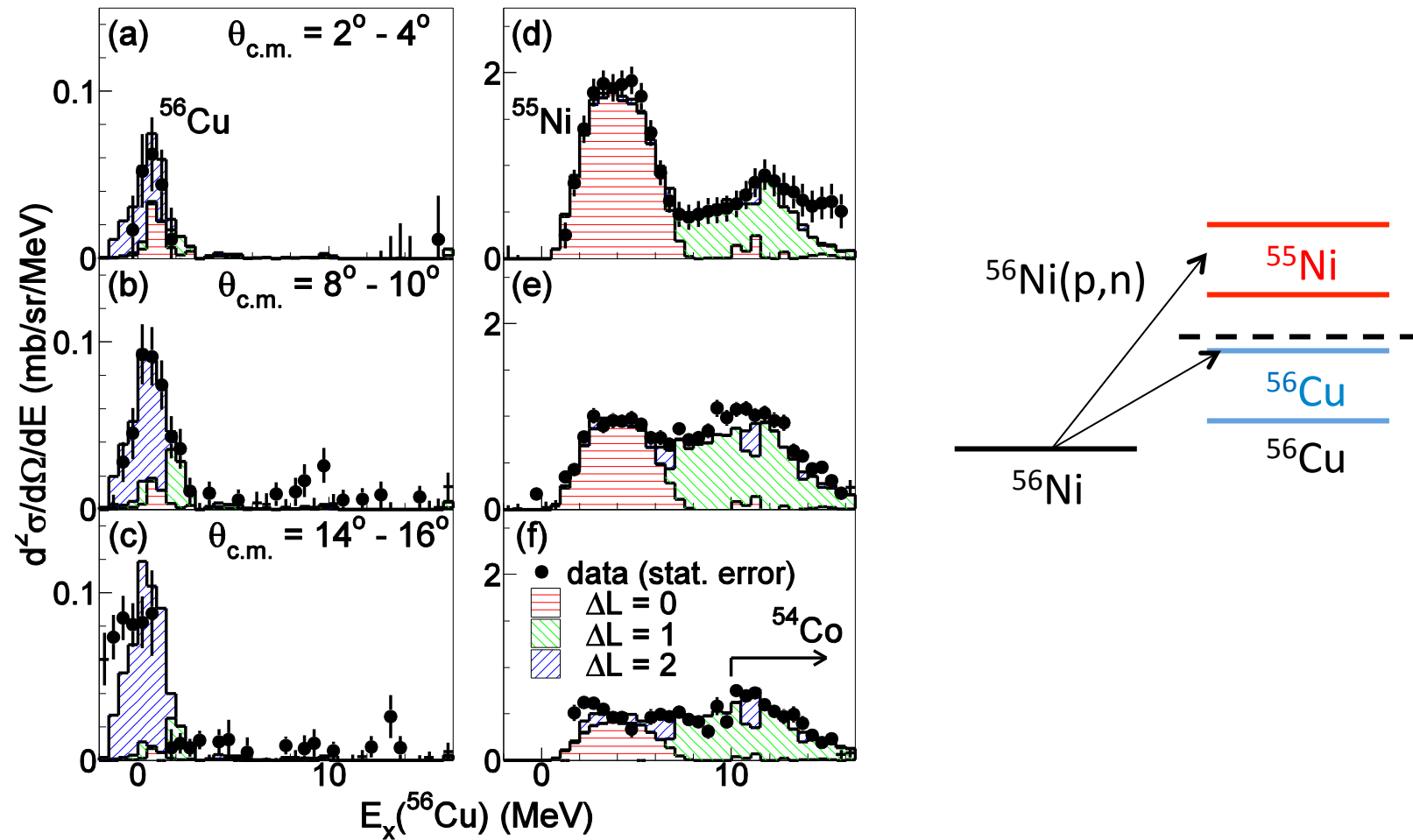


Cross sections of each multipole (ΔL)

A distorted wave impulse approximation (DWIA)

- Code : DW81
- Optical potential by Nadasen et al., Phys. ReV. C 23, 1023 (1981).
- Normal modes for transition density calculation
- NN interaction by Franey and Love, Phys. ReV. C 31, 488 (1985).

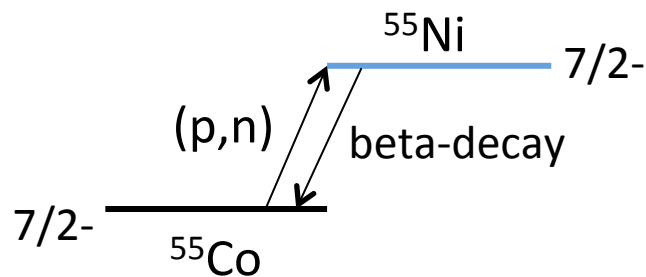
Results of MDA



GTR and SDR are extracted!

Calibration of the proportionality

$$\left(\frac{d\sigma}{d\Omega}(q=0) \right)_{(p,n)} = \hat{\sigma} B(GT)$$



Mixed :

GT of $B(GT)=0.267$

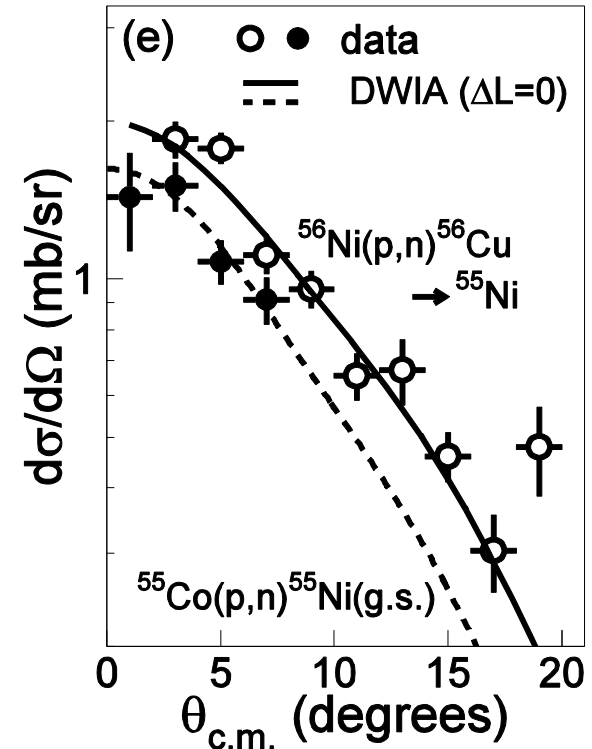
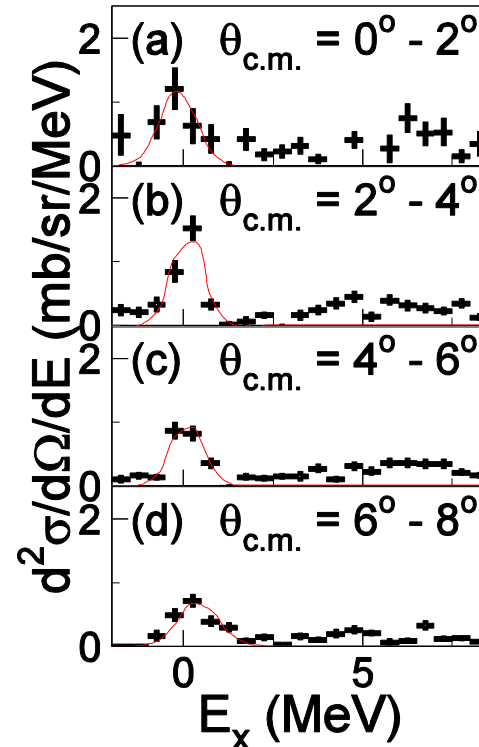
(Aysto et al., Phys. Lett. B138, 369 (1984))

Fermi of $B(F)=1$

Fraction of GT cross section : 0.51 ± 0.03

using $\hat{\sigma}_{GT} / \hat{\sigma}_F = 4.0 \pm 0.2$

Taddeucci et al., Nucl. Phys. A469, 125 (1987).



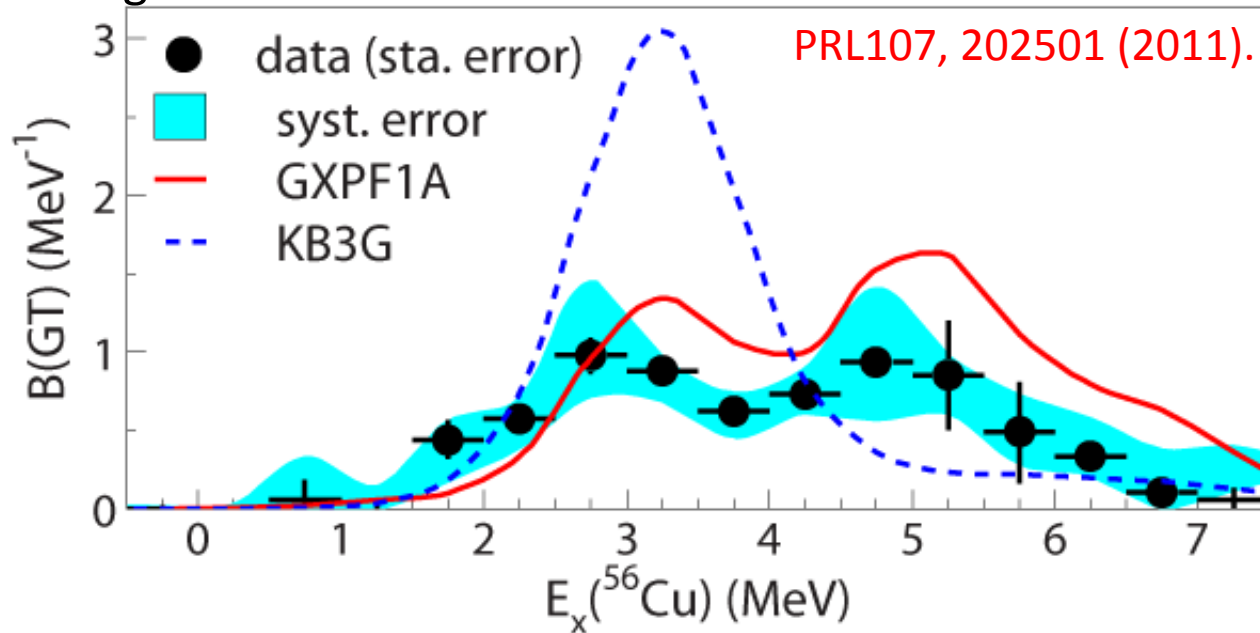
GT unit cross section of $^{55}\text{Co}(p,n)$ at 110 MeV/u

$\rightarrow 3.2 \pm 0.5$ mb/sr

\rightarrow Consistent with 3.5 ± 0.2 mb/sr
for $^{58}\text{Ni}(p,n)$ at 120 MeV

GT strengths from $^{56}\text{Ni}(p,n)$ at 110 MeV/u

- Use the extracted $\Delta L=0$ component in combination with unit cross section to extract Gamow-Teller strength [B(GT)].
- Compare with large-scale shell-model calculations



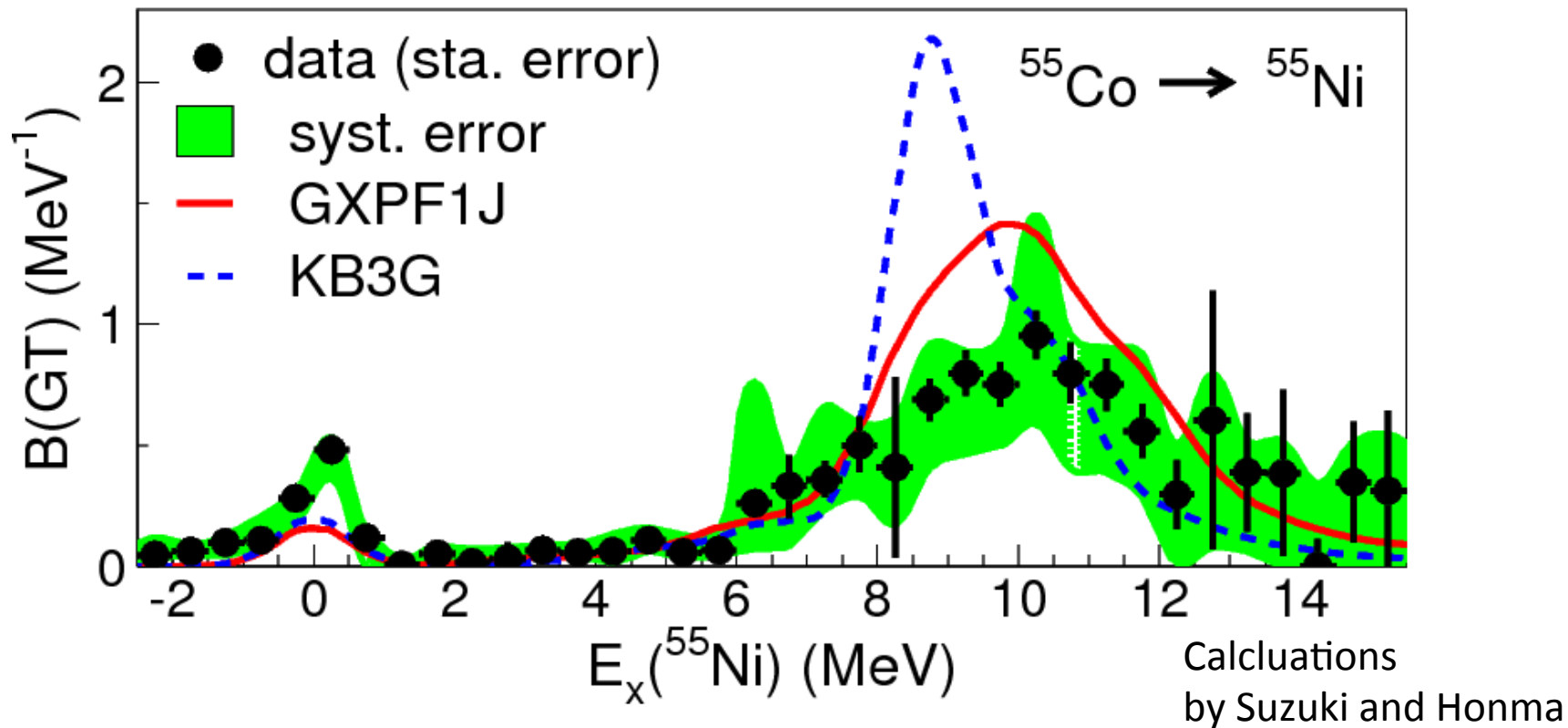
GXPF1A: Honma et al. : constrained by data in full pf-shell

KB3G: Poves et al. : less constraints – **used in database for weak rates for astrophysical purposes.**

Difference between KB3G and GXPF1A:

- KB3G weaker spin-orbit and pn-residual interactions
- KB3G lower level density

A preliminary result of ^{55}Co



KB3G : X

GXPF1"J" : O

Consistent with the comparison in ^{56}Ni

Astrophysical applications in RIKEN

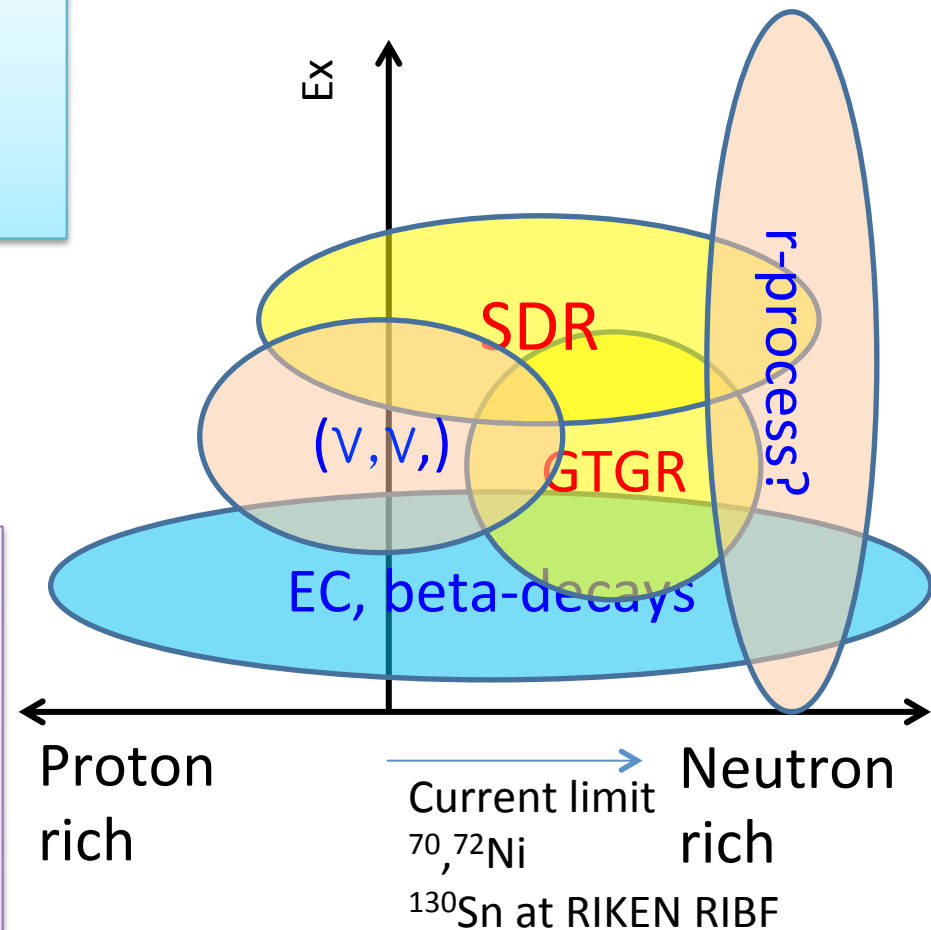
The developed technique
 + RIKEN RIBF (**intense RI beam**)
 + SAMURAI spectrometer (**efficient PID**)
 + Neutron wall (WINDS)

probe any Ex on any A/Z
 (beam intensity 10^{4-5} pps)

Better understanding of
 weak response →
 EC/beta-decays
 Neutral weak currents

e.g., Synthesis of Mn
 $^{56}\text{Ni}(\nu, \nu p)^{55}\text{Co} \rightarrow ^{55}\text{Fe} \rightarrow ^{55}\text{Mn}$
 GXPF1 \gg KB3G (a factor of 3)
 T. Suzuki et al., Phys. Rev. C79,
 061603(R) (2009).

R-process (GT + first forbidden)
 T. Suzuki et al., arXiv:1110.3886



Questions :
 Which nucleus is the key?
 How reliable is the calculation
 during the extra/interpolation?

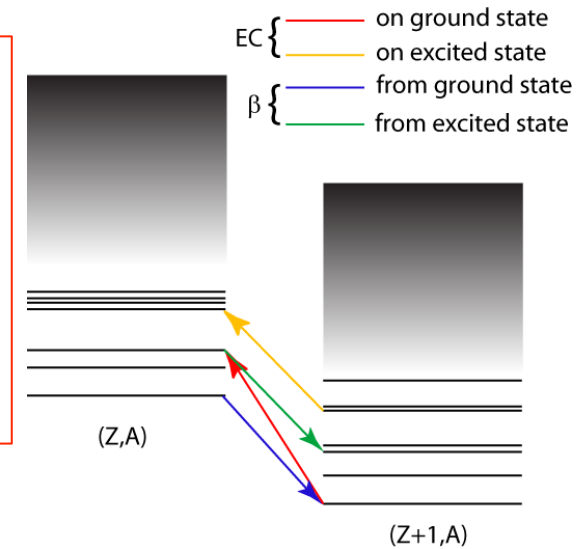
Summary and conclusion

- A new experimental technique to measure GT strengths (any E_x & (A,Z))
- The first case: ^{56}Ni (nuclear structure/astrophysics)
→ KB3G (used in astrophysical data base) : x
GXPF1A : 0
- Preliminary results for $^{55}\text{Co}(p,n)^{55}\text{Ni}$
- A lot of applications;
EC/beta-decays, Neutral weak currents, R-process
(GT + first forbidden)

Backups

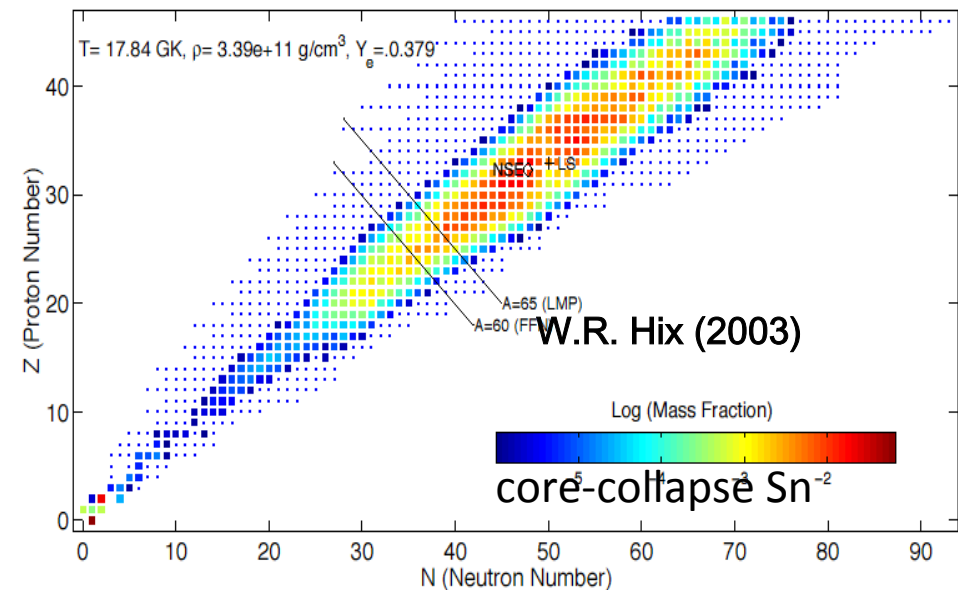
Weak reactions (electron capture) in supernovae

- Key ingredient: **Gamow-Teller strengths**
- Many nuclei play a role (A-40-120)
- Majority are unstable
- excitation can take place from excited nuclear states



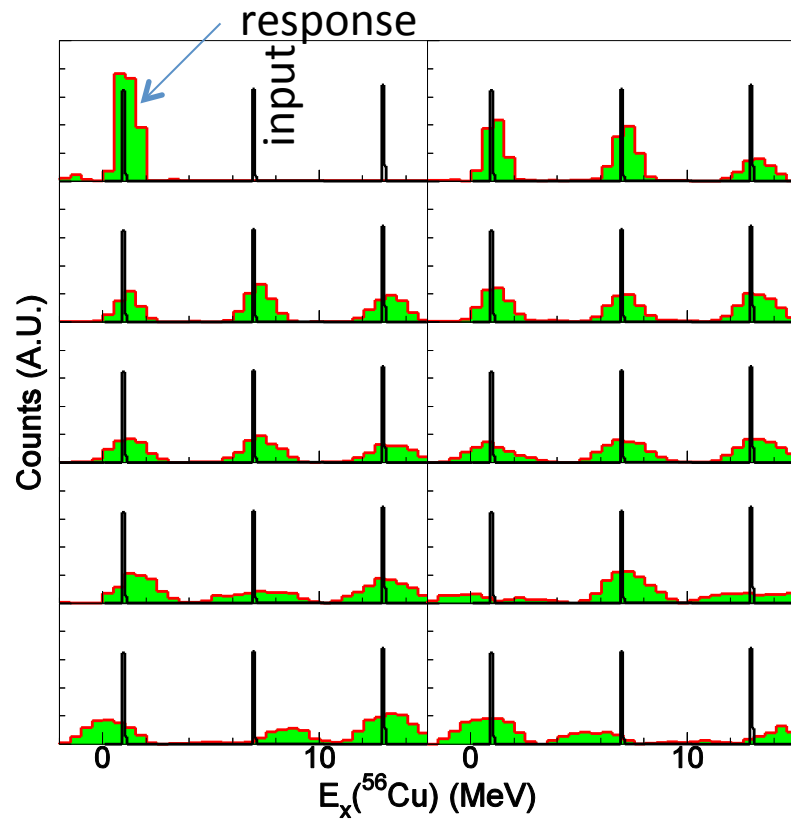
Impossible to measure even a sizeable fraction of cases

- Test theory with cases that constrain key model parameters
- Measure nuclei that are particularly abundant in supernovae

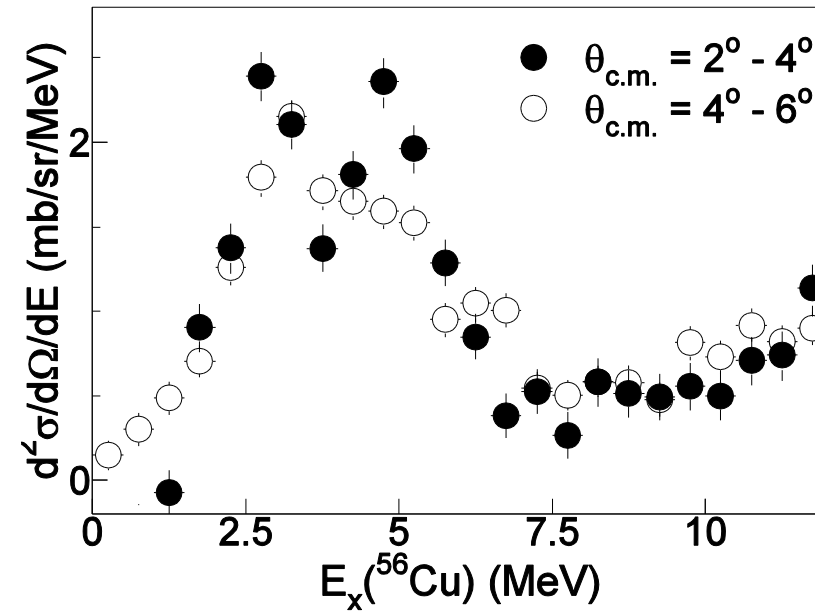


Resolution effect

Simulation

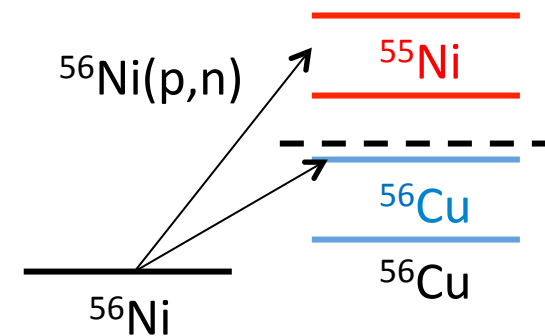
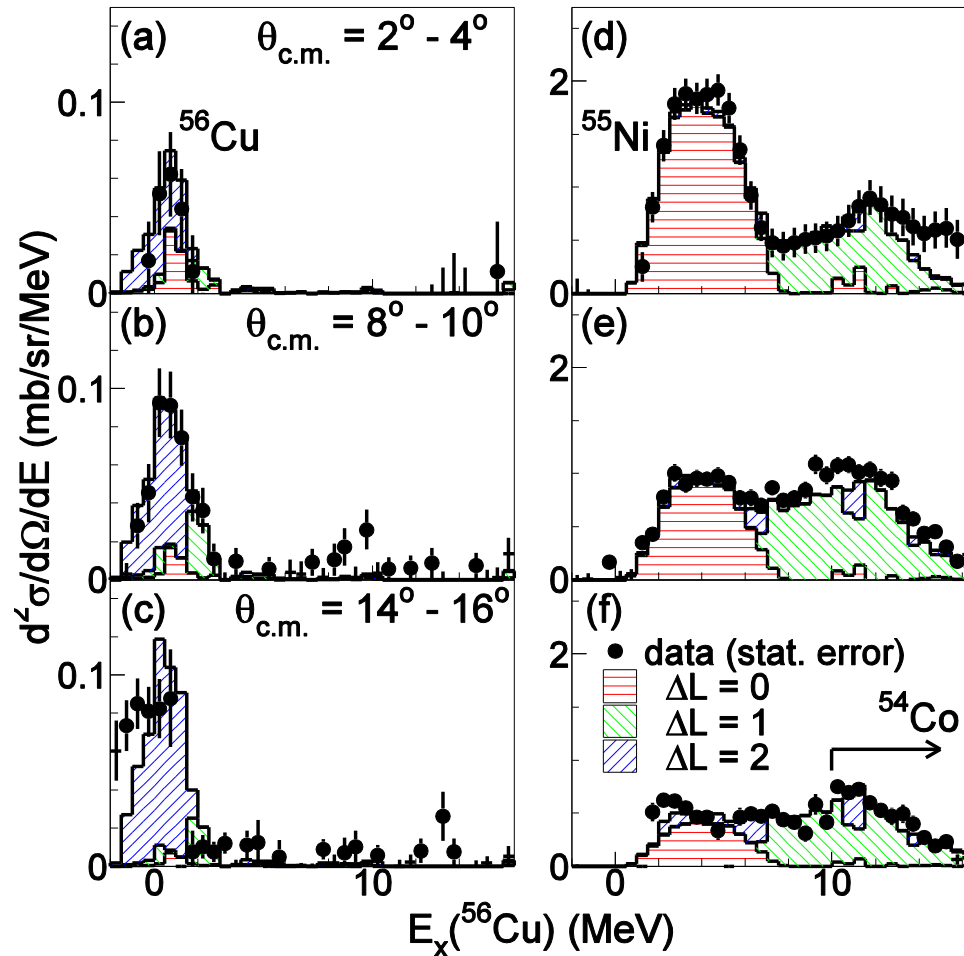


Experimental spectra



Spectra at forward angles are smeared by using simulated energy resolution.

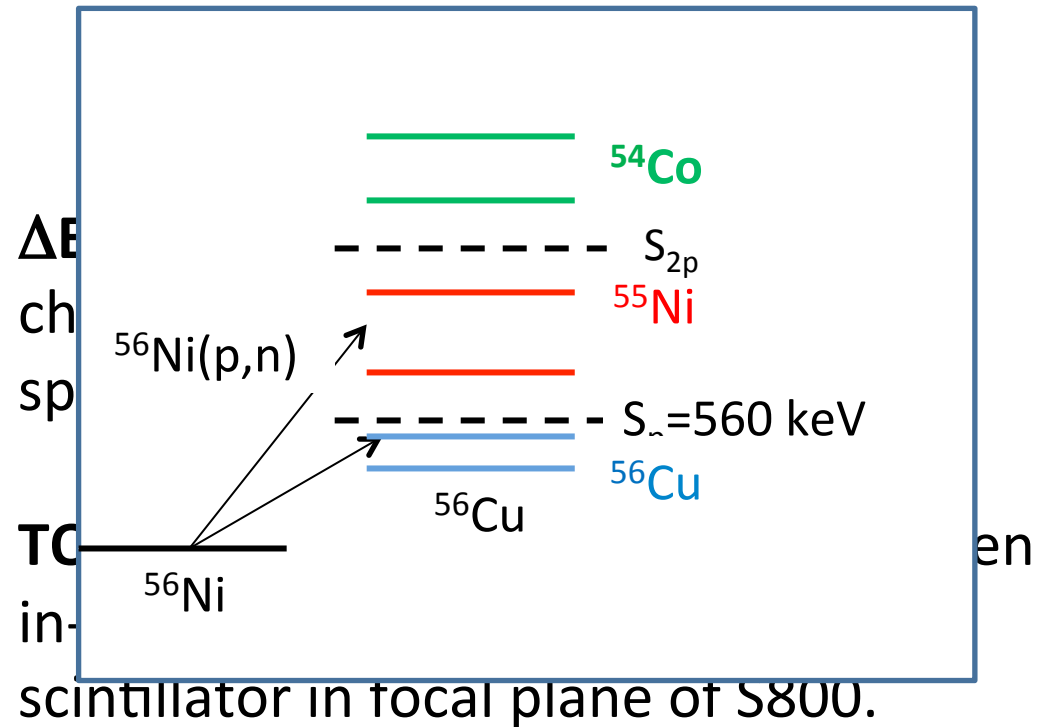
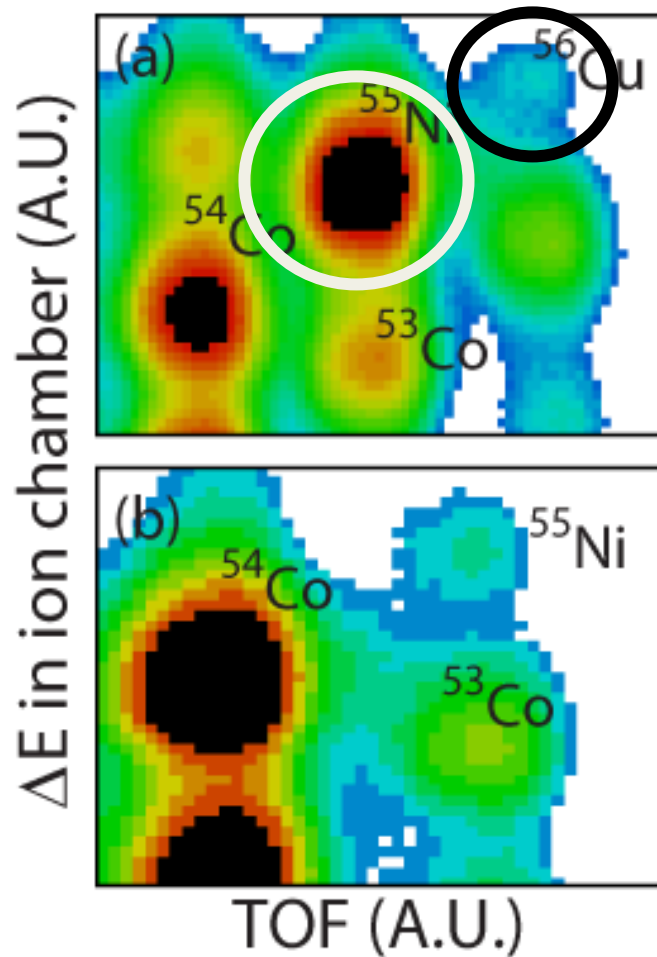
Results of MDA



GT component dominates the region below 8 MeV.
 → Scale the spectrum before smearing

Event selection in S800

^{56}Ni beam component



^{55}Co beam component

Applications of CE reactions

Nuclear Astrophysics

- weak rates for late stellar evolution
- neutrino processes
- specific weak interactions for novae

Nuclear structure

- Spin-isospin response
- test of structure models up to high excitation energies
- **Shell evolution**
- Double beta decay

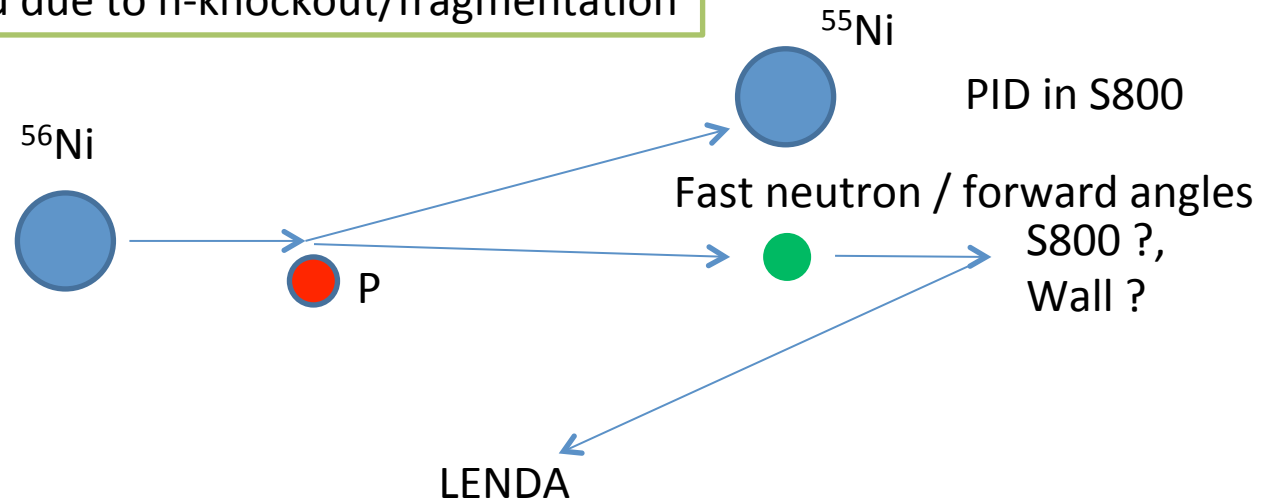
Isovector giant resonances

- macroscopic properties of nuclear matter (neutron-skin, EOS)
- microscopic descriptions high in the continuum

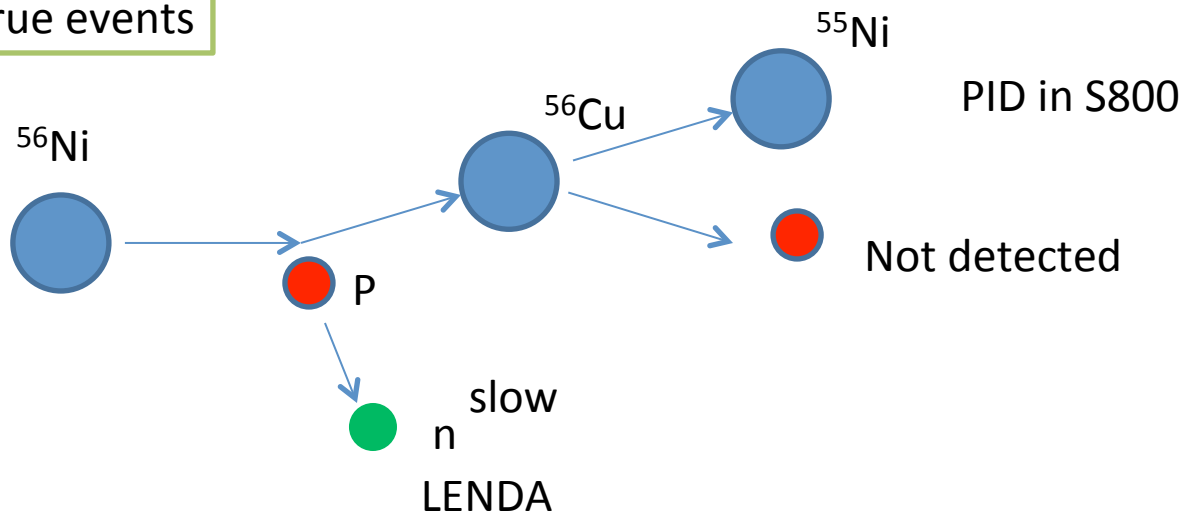
Background

due to n-knockout/frag. reactions

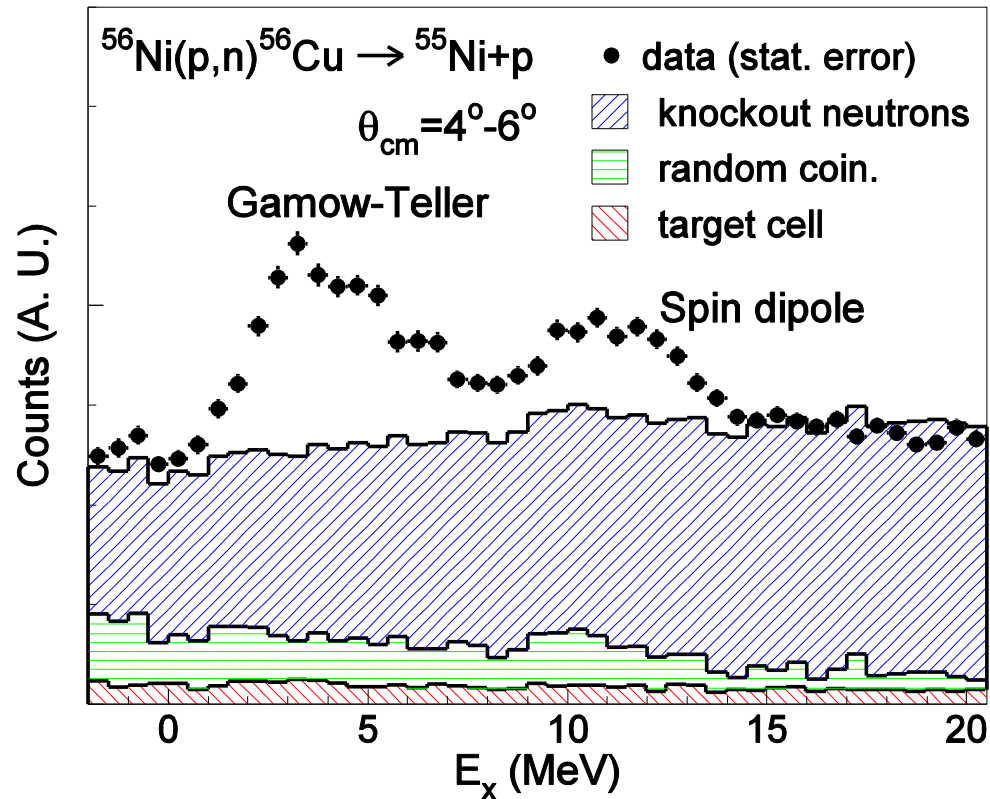
Background due to n-knockout/fragmentation



True events



Background subtraction

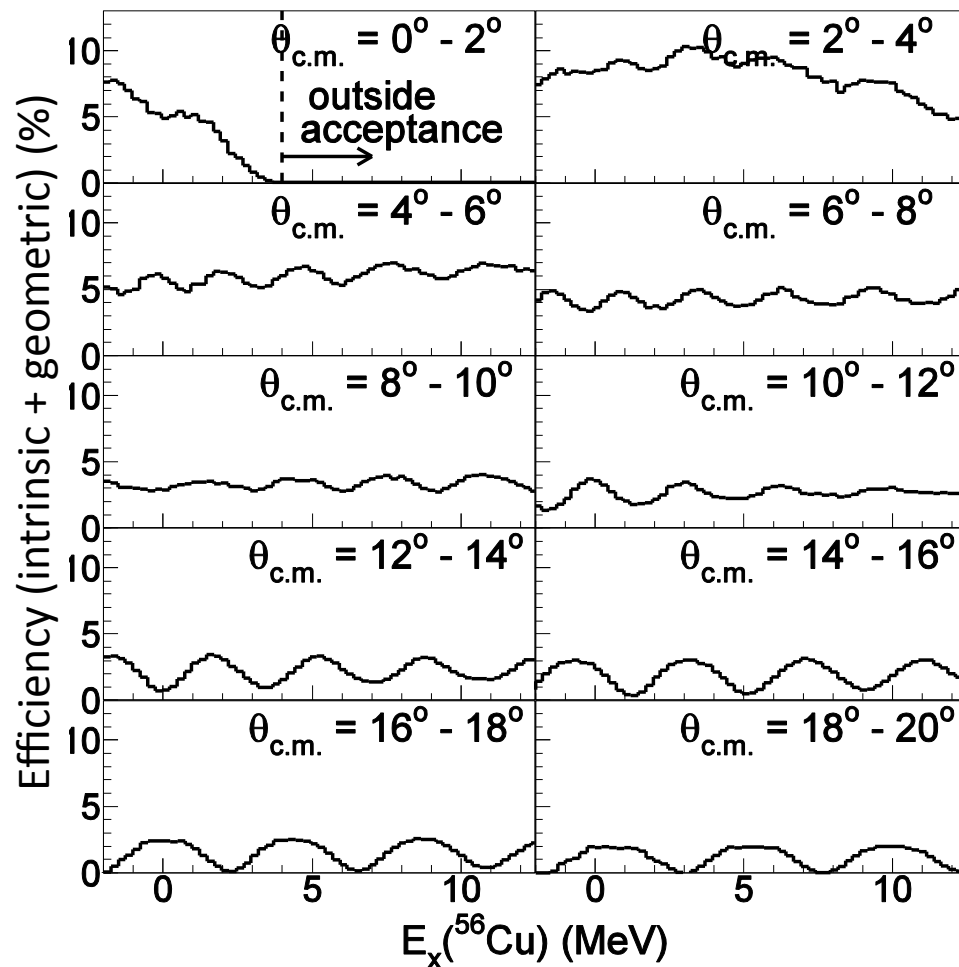
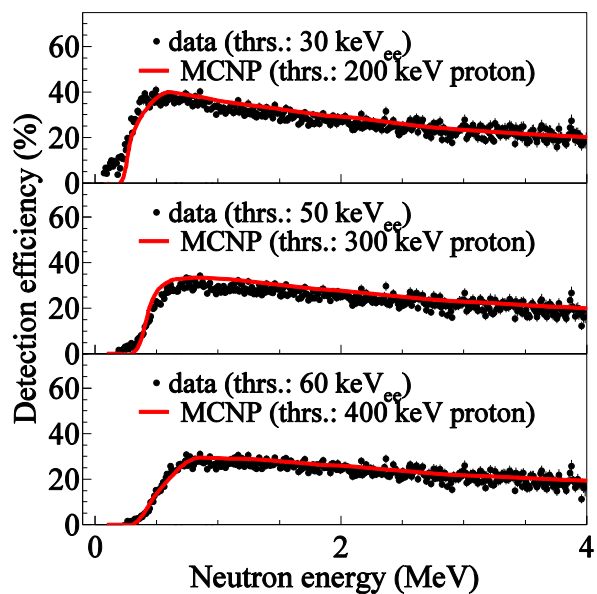
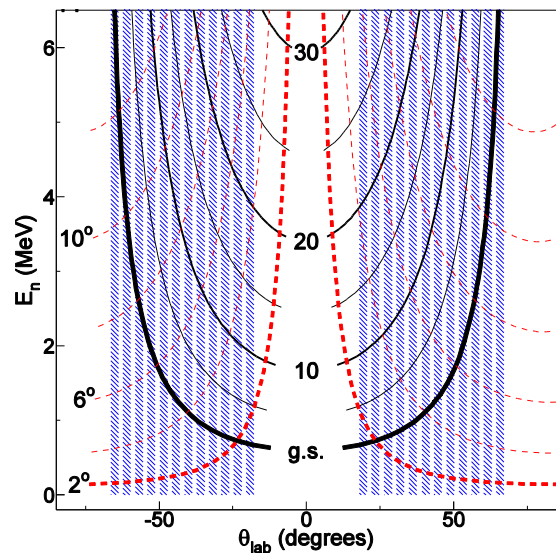


Largest source of background :
 N-knockout/frag. background
 Modeled by using
 $^{56}\text{Ni}+p \rightarrow ^{53}\text{Co} + 2p + n$
 (scaled)

Second one :
 Random background
 caused by coincidence with
 preceding beam pulse

Smallest one :
 Background due to the cell of the
 target is small
 → liquid hydrogen target system
 is important!

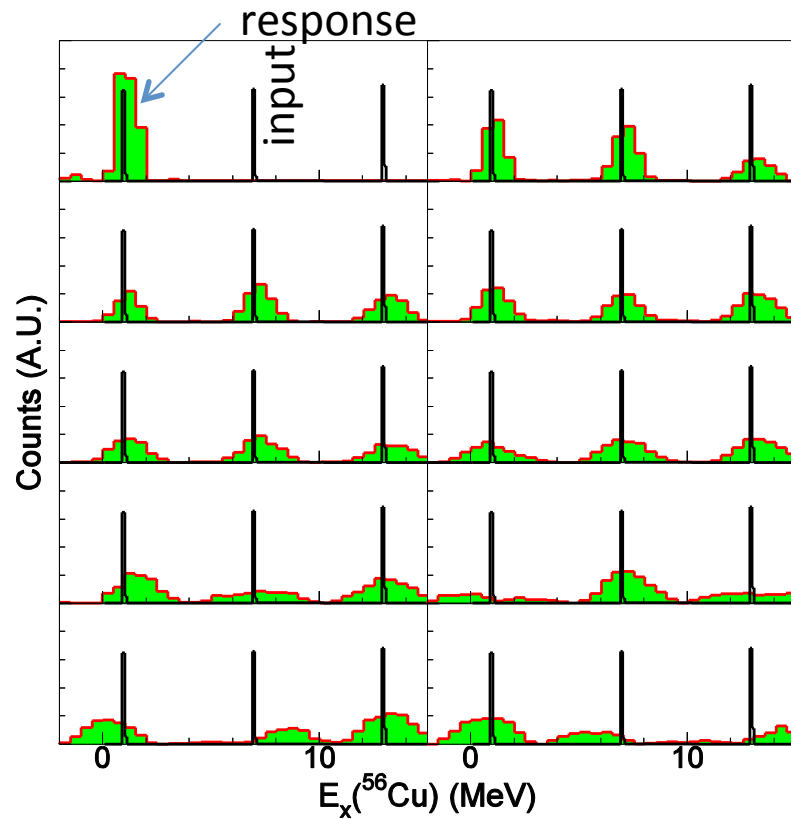
Efficiency



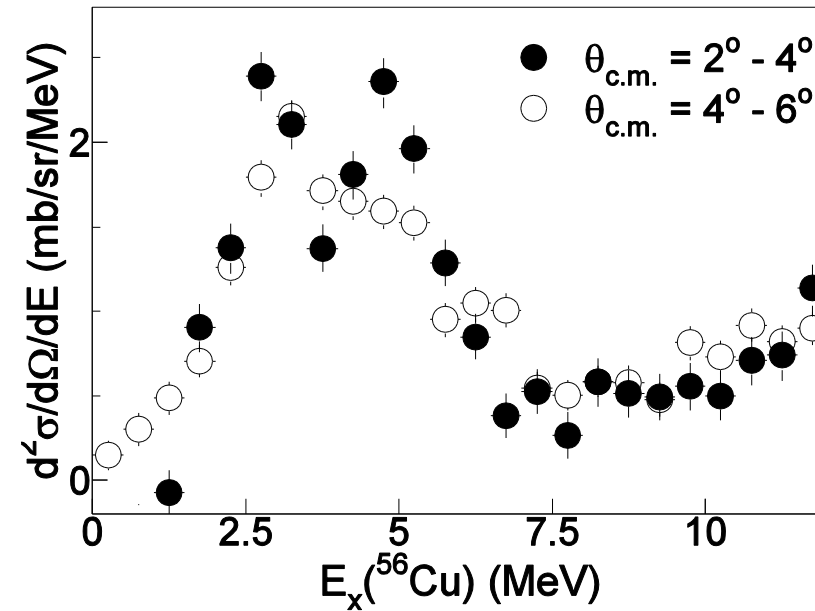
GEANT3

Resolution effect

Simulation

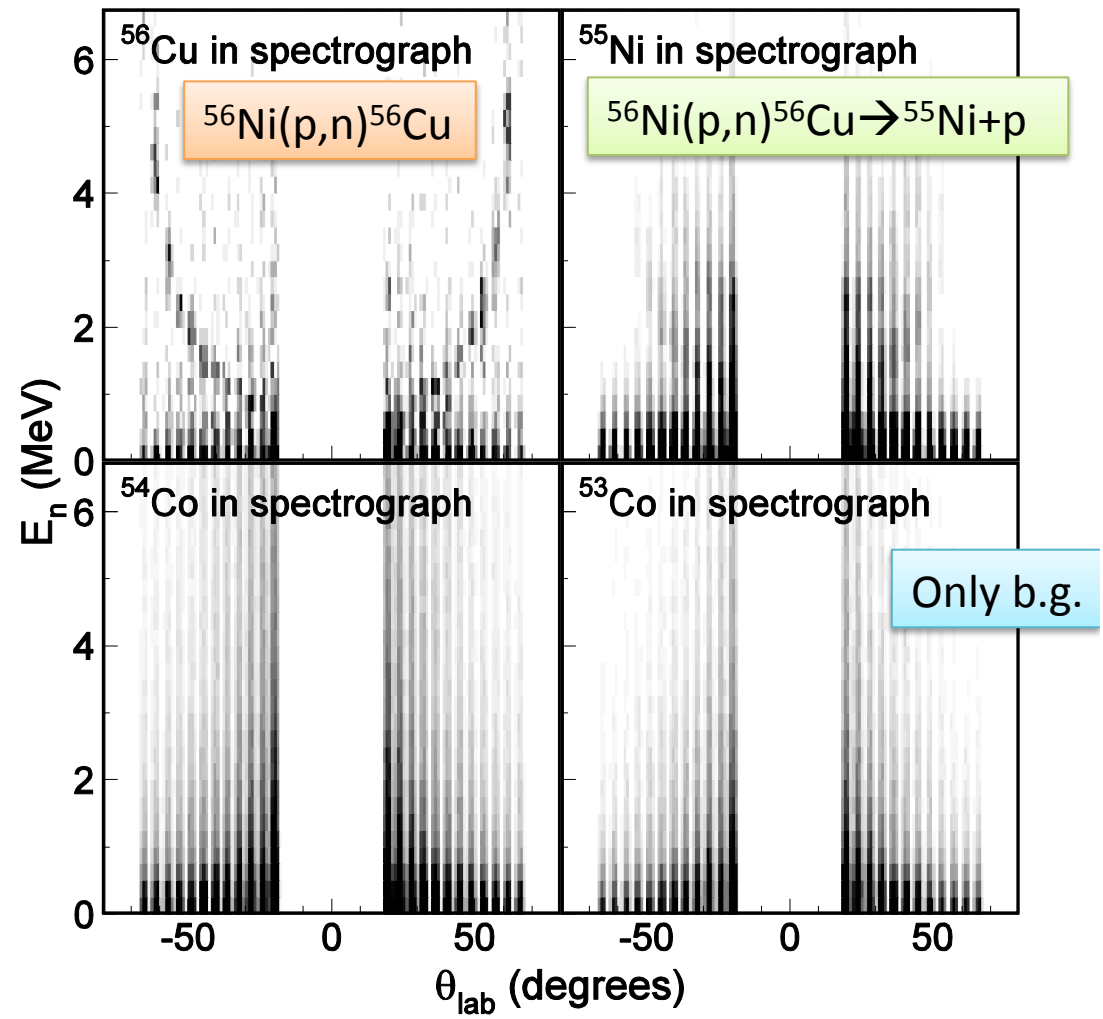
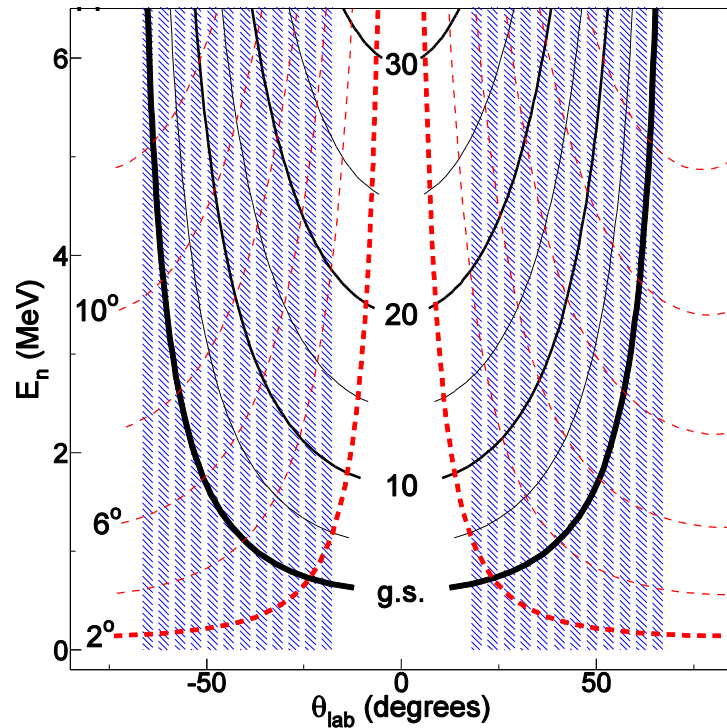


Experimental spectra

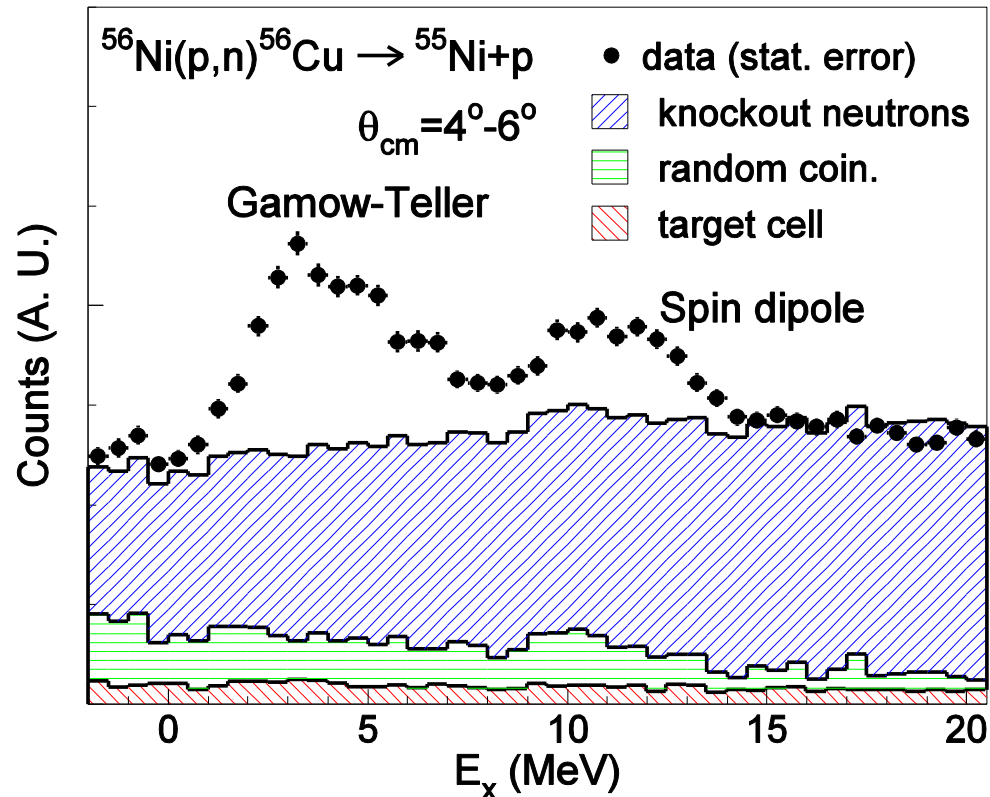


Spectra at forward angles are smeared by using simulated energy resolution.

Neutron energy spectra



Background subtraction



Largest source of background :
N-knockout/frag. background
Modeled by using
 $^{56}\text{Ni}+p \rightarrow ^{53}\text{Co} + 2p + n$
(scaled)

Second one :
Random background
caused by coincidence with
preceding beam pulse

Smallest one :
Background due to the cell of the
target is small
→ liquid hydrogen target system
is important!